Chemical Plume Tracing via an Autonomous Underwater Vehicle

Jay A. Farrell, *Senior Member, IEEE*, Shuo Pang, and Wei Li, *Member, IEEE*

***Abstract*—Olfactory-based mechanisms have been hypothesized for biological behaviors including foraging, mate-seeking, homing, and host-seeking. Autonomous underwater vehicles (AUVs) capable of such chemical plume tracing feats would have applicability in searching for environmentally interesting phenomena, unexploded ordinance, undersea wreckage, and sources of hazardous chemicals or pollutants. This article presents an approach and experimental results using a REMUS AUV to find a chemical plume, trace the chemical plume to its source, and maneuver to reliably declare the source location. The experimental results are performed using a plume of Rhodamine dye developed in a turbulent, near-shore, oceanic fluid flow.**

***Index Terms*—Autonomous underwater vehicles (AUVs), behavior-based planning (BBP), chemical plume tracing (CPT), reactive planning.**

I. Introduction

OLFACTORY-BASED mechanisms have been hypothesized for a variety of biological behaviors [1]–[3]: homing by Pacific salmon [4], foraging by Antarctic procellariiform seabirds [5], foraging by lobsters [6], [7], foraging by blue crabs [8], [9], and mate-seeking and foraging by insects [10], [11]. Typically, olfactory mechanisms proposed for biological entities combine a large-scale orientation behavior based in part on olfaction with a multisensor local search in the vicinity of the source. The long-range olfactory-based search is documented in moths at ranges of 100–1000 m [12] and in Antartic procellariiform seabirds [5].

This article presents an algorithm to replicate these chemical plume tracing (CPT) feats using an AUV. The goal for the autonomous vehicle is to locate the stationary source of a chemical that is transported in a turbulent fluid flow. The basic idea of CPT is illustrated in Fig. 1. A vehicle is constrained to maneuver within a region referred to as the OpArea. Within the OpArea the AUV should search for a specified chemical, for which a binary sensor is available. The mission starts with the AUV searching the OpArea for the chemical plume. A binary sensor outputs 1.0 if the chemical concentration is above threshold or 0.0 if the chemical concentration is below threshold. If above threshold chemical is detected, the AUV should trace the chemical plume to its source and accurately declare the source location. Following the source declaration, additional AUV maneuvers might be desired to acquire additional data, possibly using auxiliary sensors. Such AUV capabilities have applicability in searching for environmentally interesting phenomena, hazardous chemicals, and pollutants. The plume depicted in Fig. 1 is greatly simplified. Realistic plumes may meander, are intermittent or patchy distributions of chemical, and do not have a uniformly increasing width as a function of the distance from the chemical source.

An initial approach to designing an autonomous AUV plume-tracing strategy might attempt to calculate a concentration gradient, with subsequent plume tracing based on gradient following; however, gradient-based algorithms are not feasible in environments with medium to high Reynolds numbers [13]–[18]. At medium and high Reynolds numbers, the evolution of the chemical distribution in the flow is turbulence dominated [15]. The result of the turbulent diffusion process is a highly discontinuous and intermittent distribution of the chemical [13], [19]. A dense array of sensors distributed over the area of interest and a long (i.e., several minutes) time-average of the output of each sensor is required to estimate a smooth (time-averaged) chemical distribution [20], [21] suitable for gradient-based calculations. However, the required dense spatial sampling and long time-averaging makes such an approach inefficient for implementation on an AUV. In addition, even decameters from the odor source in the direction of the flow the gradient is too shallow to detect in a time-averaged plume. Therefore, gradient following is not practical.

The instantaneous odor distribution is distinct from the time-averaged plume [13], [14]. The major differences include: the time-averaged plume is smooth and unimodal while the instantaneous plume is discontinuous and multimodal; the time-averaged plume is time invariant while the instantaneous plume is time-varying. Instantaneous concentrations well above the time-averaged concentration will be detected much more often than predicted by the time-averaged plume model. The fact that instantaneous chemical concentrations well above the time average are available at significant distances from the source is one of reasons that olfaction (i.e., a chemical detection based method) is a useful long distance sensor [22]. A challenge in using olfaction on AUVs is to design effective algorithms to determine the odor source location even though the odor source concentration is not known, the advection distance of the detected odor is unknown, and the flow varies with both location and time.

Manuscript received October 27, 2003; revised July 12, 2004; accepted September 13, 2004. This work was supported in part by the U.S. Office of Naval Research Grant ONR N00014-98-1-0820 under the ONR/DARPA Chemical Plume Tracing Program and N00014-01-1-0906 under the ONR Chemical Sensing in the Marine Environment Program. Both programs were led by K. Ward of ONR. Associate Editor: D. Blidberg.

J. A. Farrell and S. Pang are with the Department of Electrical Engineering, University of California, Riverside, CA 92521 USA (e-mail: farrell@ee.ucr.edu; spang@ee.ucr.edu).

W. Li is with the Department of Computer Science, California State University, Bakersfield, CA 93311 USA (e-mail: wli@cs.csubak.edu).

Digital Object Identifier 10.1109/JOE.2004.838066

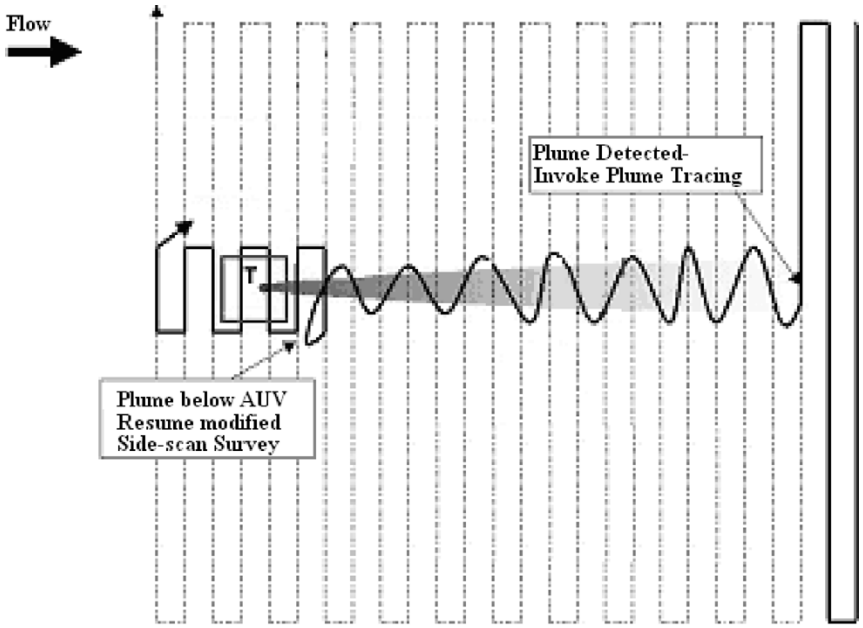

Fig. 1. A prototype CPT mission with postdeclaration maneuvering. The depicted plume is a rendition that does not attempt to include intermittency or meander.

Various studies have developed biomimetic robotic plume-tracing algorithms based on olfactory sensing. Belanger and coauthors [23], [24] presented plume tracing strategies intended to mimic moth behavior and analyzed the performance in a computer simulation. Grasso *et al.* [25], [26] evaluated biomimetic strategies and challenge theoretical assumptions of the strategies by implementing biomimetic strategies on their robot lobster. Robots intended to replicate biological approaches for plume tracing are also described in [27]–[30]. Li *et al.* [15] developed, optimized, and evaluated counterturning strategies inspired by moth behavior. The fundamental aspects of these research efforts are sensing the chemical, sensing or estimating the fluid velocity, and generating a sequence of searcher speed and heading commands such that the resulting motion is likely to locate the odor source. In each of these articles, the algorithms for generating speed and heading commands use only instantaneous (or very recent) sensor information. Typical orientation maneuvers include: sprinting upflow upon detection, moving crossflow when not detecting, and manipulating the relative orientation of a multiple sensor array, either to follow an estimated plume edge or to maintain the maximum mean reading near the central sensor.

This paper extends plume tracing research by presenting a complete strategy for finding a plume, tracing the plume to its source, and maneuvering to accurately declare the source location; and, by presenting results from successful, large-scale, in-water tests of this strategy. The assumptions made herein relative to the chemical and flow are that the chemical is a neutrally buoyant and passive scalar being advected by a turbulent flow. The AUV is capable of sensing position, concentration, and flow velocity. The concentration sensor is used as a binary detector (above or below threshold). We solve the plume-tracing problem in two dimensions. A main motivation for implementing the algorithms in two dimensions is the computational simplification achieved; however, neutral buoyancy of the chemical or stratification of the flow [31] will often result in a plume of limited vertical extent, which may be approximated as two-dimensional.

II. Behavior-Based Planning (BBP): Review and Overview

A BBP strategy is an efficient means to navigate an autonomous system in an uncertain environment. A *behavior* is a mapping of sensor inputs to a pattern of motor actions. To use a set of behaviors to achieve a task a mechanism for coordinating the behaviors is also required.

In the late 1970s and early 1980s, Arbib began to investigate models of animal intelligence from the biological and cognitive sciences point-of-view to gain alternative insight into the design of advanced robotic capabilities [32]. At nearly the same time, Braitenberg studied methods by which machine intelligence could be evolved by using sensor-motor pairs to design vehicle systems [33]. Later, a new generation of AI researchers began exploring the biological sciences in search of new organizing principles and methods of obtaining intelligence. This research resulted in the reactive behavior-based approaches. Brooks' subsumption architecture is the most influential of the purely reactive paradigms. Its basic idea is to describe a complex task by several behaviors, each with simple features [34]. Design of a behavior-based planner includes two significant steps. First, the designer must formulate each reactive behavior quantitatively and implement the behavior as an algorithm. Second, the designer must define and implement a methodology for coordinating the possibly conflicting commands from the different behaviors to achieve good mission performance.

Various coordination approaches have been proposed. For example, each behavior can output a command and a priority. Traditional binary logic can be used to select and output the command with the highest priority. An alternative coordination approach is to use artificial potential fields [35]. A drawback to

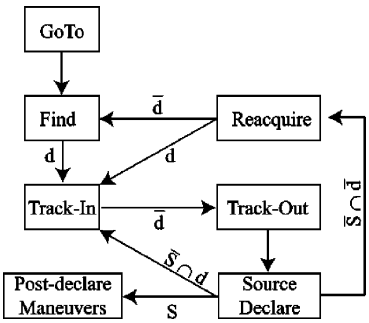

Fig. 2. Behavior switching diagram. The symbol d denotes a behavior switch that occurs when chemical is detected. The symbol $\overline{d}$ denotes a behavior switch that occurs when chemical is not detected prior to the end of the behavior. S indicates that the source location has been declared. $\overline{S}$ indicates that the source location has not been declared.

either approach is that formulating and coordinating the reactive behaviors requires significant premission simulation and testing. These are *ad hoc* processes and may need to be readdressed each time new behaviors are added or existing behaviors are changed. In some applications, these tuning parameters depend heavily on environmental conditions. Another alternative that has been suggested is to train an artificial neural network (ANN) to perform the behavior coordination [36]. However, this approach would require some mechanism for determining correct coordination decisions for each training scenario and would provide no guarantee that all coordination situations are properly trained [37]. Fuzzy logic can improve the performance of reactive behavior coordination [36], [38], [39] by providing a formalism for automatically interpolating between alternative behaviors.

Behavior based design methodologies are bottom-up approaches to the design of an intelligent system. Observed behaviors with simple features are analyzed and synthesized independently. In this paper, we describe the behaviors and coordination mechanism that were used to solve the problem of CPT for an AUV. The CPT strategy was inspired by behaviors observed in biological entities. Detailed simulation analysis of this and alternative biomimetic strategies and analysis of performance as a function of parameter settings is presented in [15].

III. CPT BBP Design

Fig. 2 displays the behaviors and switching logic used to implement CPT algorithms using BBP. In Fig. 2, S and d are Boolean variables. The symbols S and $\overline{S}$ indicate that the source location has or has not been declared, respectively. The symbol d indicates that chemical has been detected. The symbol $\overline{d}$ indicates that the behavior completed without detecting chemical. Prior to source declaration, whenever chemical is detected, the Track-In behavior is triggered. Due to the intermittency caused by the turbulent flow, an instantaneous chemical reading below the detection threshold does not necessarily imply that the AUV is out of the plume. Therefore, the sequence of behaviors Track-Out, Reacquire, Find is instantiated as the time since the last detection increases. The specific aspects of each behavior and the logic for switching between the behaviors are described in the following subsections. The planner is implemented on a PC104 computer that will be referred to as the adaptive mission planner (AMP).

TABLE I
Pseudocode for Track-In Behavior

```
Behavior::track_in( )
{
  v = v_c ;
  if(odor conc. >= threshold)
  { // Stay in track in
     ψ_c = ψ_f + 180 + LHS*β;
     if (lim(ψ_v - ψ_f,-180,180) > 0)
      LHS =1;
     else
      LHS =-1;
     T_last = t;
     last_detection_point = position;
  }
  else if((t - T_last) > λ)
  { // Go to track out
   // save last detection point
   lost_pnts[i]=last_detection_point;
   i++;
   return track_out;
  }
  return track_in;
}
```

A. CPT Behaviors

1) Go-To: The Go-To behavior is used to drive the AUV to a desired location. This is used for example at the start of a mission to maneuver the AUV to a desired starting location within the OpArea and at the end of the mission to maneuver the AUV to a desired rendezvous location. The Go-To behavior directly executes the Go-To guidance command (see Appendix A).

2) Find: Since there is no prior information about the location of the source, the AUV may be required to search the entire OpArea. Since the odor plume will be downflow from the source, the search is designed to start at the most downflow corner of the OpArea. From this starting location, the AUV should proceed across the flow until it either reaches a boundary of the OpArea or detects chemical. Although the largest component of the commanded velocity is across the flow, there must also be a component either up or down the flow so that the AUV will explore new locations in the OpArea. If odor is detected, then the behavior switches to Track-In. If the AUV meets the boundary without detecting odor, then four candidate directions are computed as $\psi_{\mathrm{f}} \pm 90 \pm 20$, where ψ_{f} is the flow direction in degrees. Of these four candidate directions, the behavior selects the direction that maintains the same sign of the velocity along the boundary and reverses the sign of the velocity perpendicular to the boundary. When none of the four candidates satisfies this condition, then the motion is continued parallel to the boundary until the condition is achieved or another boundary is met. At such a corner, two directions of motion must be changed, and the solution can always be found. When the flow is parallel to a boundary, then this Find strategy results in a billiard ball type of reflection at the OpArea boundary.

3) Track-In: Studies described in [15] show that immediately following a chemical detection, good plume tracking performance is attained by driving at an angle $\beta \in [20, 70]$ deg. offset relative to upflow. When driving at a nonzero angle β offset relative to upflow and contact with the plume is ultimately

TABLE II
PSEUDOCODE FOR TRACK-OUT BEHAVIOR. F IS A UNIT VECTOR IN THE DIRECTION OF THE FLOW. F_p IS ROTATED POSITIVELY BY 90 DEG. RELATIVE TO F IN THE HORIZONTAL PLANE. R, L_u, AND L_c ARE POSITIVE CONSTANTS

```
Behavior:: track_out( )
{
   v = v_c ;
   if(odor conc. >= threshold)
   {
    init = 1;
    S = src_chck(lost_pnts);
    if(S)
       return post_dclr;
    else
       return track_in;
   }
   else
   {
    if(init==1)
    {
     UP = upflow pnt in lost_pnts
     init = 0;
     pnt=UP - L_u*F - L_c*LHS*F_p;
    }
    if(‖veh_pos -pnt‖<R)
    {
      init = 1;
      S = src_chck(lost_pnts);
      if(S)
       return post_dclr;
      else
       return reacquire;
    }
    else
      goto(pnt);
   return track_out;
   }
}
```

lost, the AUV can predict which side of the plume it exited from and perform a counterturn to reacquire the plume. Such counterturning strategies are exhibited in several biological entities. The Track-In behavior implements an engineered version of such a strategy.

Pseudocode for the Track-In behavior is contained in Table I. The AMP will stay in Track-In mode as long as there has been an above threshold concentration sensed in the last λ seconds. While chemical is being detected, AMP adjusts the commanded heading ψ_{c} to be offset by $\mathrm{LHS} \star \beta$ relative to the upflow direction $\psi_{\mathrm{u}} = \psi_{\mathrm{f}} + 180$. In this expression β is a constant and LHS is a variable that switches based on the relative directions of the AUV and flow. LHS is 1 if we expect the AUV to drive out of the plume from the left side (when looking upflow) of the plume. Otherwise, LHS is -1. In Table I, the function '$\lim(x, -180,180)$' adds or subtracts to x the multiple of 360 deg required so that the result is between -180 and 180 deg. Each time chemical is detected, the current AUV position is saved; therefore, when Track-In exits, the last detection point is available and saved in a list named lost_pnts.

As long as the AUV is detecting chemical at least every λ seconds, it will make upflow progress. The actual AUV trajectory will include small angle, counterturning oscillations relative to the upflow direction. If the AUV fails to detect chemical for λ seconds, then AMP saves the last detection point (at most 6 points are saved) and switches to Track-Out.

4) Track-Out: Pseudocode for the Track-Out behavior is contained in Table II. When the AMP switches to Track-Out, it has detected chemical slightly more than λ seconds previously; in addition, there will be at least one point on the list of last detection points. Normally, the most recent detection point will be the last one on the list; however, since other behaviors manipulate the list, this is not guaranteed. Also, the variable LHS indicates on which side of the plume the AUV was located when contact with the plume was lost.

TABLE III
PSEUDO CODE FOR REACQUIRE BEHAVIOR

```
Behavior::reacquire( )
{
 if(odor conc. < threshold){
   pnt= find_upflow_lost_pnt();
   if(n < N_re){
     center_pnt=pnt -
       10(N_re-1-n)/(N_re-1)*F;
     if(bow_tie(center_pnt)== done)
       n++;
     }
    else{
      n = 0;
      remove_pnt_from_list(pnt);
      if(lost_pnt_list_is_empty())
        return find;
    }
    return reacquire;
 }
 else{
   n = 0;
   return track_in;
 }
}
```

The Track-Out behavior attempts both to make progress toward the source (upflow) and to quickly reacquire contact with the plume. To accomplish these two objectives, AMP commands the AUV to go to a point that is L_u meters upflow and L_c meters across the flow from the most upflow point on the list of lost detection points. The crossflow direction is selected so that, if chemical is not detected, the AUV is expected to end up on the opposite side of the plume, since crossing the plume increases the likelihood of detecting chemical. Track-Out ends either when chemical is detected or the AUV arrives at the commanded location. In either case the BBP checks whether it can declare a source location prior to determining the next maneuver. If the source is declared, then postdeclaration maneuvering begins. If chemical is detected and the source location cannot be declared, then the behavior switches to Track-In. In this case, the AUV is at a location further up the plume than the previous most upflow detection point. If the AUV arrives at the commanded point without detecting and the source location cannot be declared, then the behavior switches to Reacquire.

5) Reacquire: Pseudo-code for the Reacquire behavior is contained in Table III. When the AMP switches to Reacquire, it has not detected chemical for several seconds; however, there will be at least one point on the list of lost detection points. Also, the variable LHS indicates the side of the plume on which the AUV was when it lost contact with the plume. To switch to the Reacquire behavior, the Track-Out behavior must have completed without detecting chemical. Therefore, several scenarios could have occurred.

- The AUV could be upflow from the source.

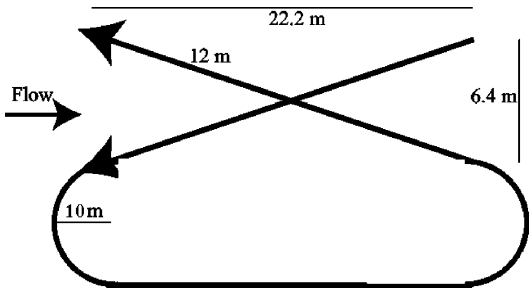

Fig. 3. Illustration of the BOWTIE maneuver used during the Reacquire maneuver. The image is not to scale.

- The AUV could have crossed the (intermittent) plume without detecting chemical.
- If the LHS variable was incorrect, then the AUV would have moved further across the flow in the direction away from the plume.

In any of these cases, the AUV should next maneuver relative to the most upflow detection point. This Reacquire maneuver must be achievable by the AUV and useful in any of the three circumstances.

The maneuver that we designed, referred to as a Bowtie, is depicted in Fig. 3. The Bowtie maneuver first tracks a line that starts on the side of the plume on which we estimate that the AUV is located. This line is angled -15 degrees relative to upflow. The upflow 15 degree angle is small enough so that the transition to Track-In is smooth, if chemical is detected. If that line completes without a detection, then the AUV transitions to the start of a second line that passes through the same center point, but has an angle of 15 degrees relative to upflow. In Fig. 3, the narrow lines indicate distances while the wide lines show the nominal AUV trajectory. If the Bowtie completes without a detection, then the last line would be followed by a clockwise turn toward downflow, which would have a radius of 10.0 m. Therefore, this maneuver explores at least 23 m on each side of its center in the direction perpendicular to the flow.

The Reacquire behavior will perform at most $\mathrm{N\_re}\,(>1)$ repetitions of the Bowtie in the vicinity of a single point on the lost point list. The first Bowtie is centered 10 m upflow from the most upflow point on the list of lost detection points. The last Bowtie is centered on the most upflow point on the list of lost detection points. The remaining (N_re-2) Bowtie centers are equally spaces between the first and last centers.

If this sequence of N_re Bowties completes without chemical detection, then the behavior removes the most upflow point from the list of last detection points. It then repeats the behavior at the most upflow point on the remaining list. This process repeats until a detection occurs or the list becomes empty. A detection at any time switches the behavior to Track-In. If the list becomes empty, then the AUV reverts to the Find behavior.

If the AUV started the Reacquire behavior upflow from the source, the shape of the Bowtie repetitions, as the center point moves downflow toward the most upflow point on the lost_pnt list, provides useful information for accurately declaring the source location. If the AUV starts the Reacquire behavior after crossing the plume without detecting, the repetitions of the Bowtie give the AUV several more chances to detect odor. If the AUV starts the Reacquire behavior across the flow from the plume, the repetitions of the Bowtie, at and upflow from the most upflow lost detection point, will bring the AUV back toward the location where the plume is likely to be. The Bowtie is sufficiently wide so that it is able to recontact the plume as long as the plume has meandered across the flow less than 13 m away from the most upflow lost detection point.

6) Cage: The Cage behavior has two responsibilities related to the safety of the AUV. First, it should prevent the AUV from leaving the operating area or return the AUV to the operating area if it has left the operating area. Second, if the AUV is more than 30 m outside the operating area, then the Cage must abort the mission. Aborting the mission in the latter case is straightforward.

When the AUV is outside the OpArea or is near (within 5 m) an edge, we find the outward unit normal $\mathrm{N} = [\mathrm{N_e}, \mathrm{N_n}]$ and the distance δ to the nearest edge. In this notation, $\mathrm{N_e}$ and $\mathrm{N_n}$ are the east and north components of the unit normal vector. If the AUV is inside the OpArea (i.e., $0 < \delta < 5$), then the commanded heading that results from the CPT algorithm is modified to remove a portion of its outward component

$$\begin{aligned} \mathrm{V} &= [\cos(\psi_\mathrm{c}), \sin(\psi_\mathrm{c})] \\ \mathrm{T} &= \mathrm{V} - \left(1 - \frac{\delta}{5}\right)(\mathrm{V^T N})\mathrm{N} \\ \psi_\mathrm{c} &= \mathrm{atan2}(\mathrm{T_e}, \mathrm{T_n}) \end{aligned}$$

where atan2 is the four quadrant arc tangent function and $\mathrm{T} = [\mathrm{T_e}, \mathrm{T_n}]$. Therefore, when inside the OpArea, the AUV should not drive itself out of the OpArea; however, a navigation fix[1] could instantaneously change the computed AUV position to be outside of the OpArea. If the AUV is outside the OpArea, then the heading command is

$$\psi_\mathrm{c} = \mathrm{atan2}(-\mathrm{Ne}, -\mathrm{N_n}).$$

B. Declaration Decision

The source declaration is not a separate behavior. Instead, it is a function that is called at the end of the Track-Out behavior. Each time that the Track-In ends, the last detection point is added to the lost_pnt list. That list is sorted according to distance along the direction of the flow. As long as the AUV is making progress up the plume, the first points on the list will be widely separated. When the AUV is near the source, the plume tracing maneuvers will cause several points on the list to be very near each other in the direction of the flow. When the first three points on the sorted list differ in the direction of the flow by less than 4 m, then the most upflow point on the list is declared as the source location. An additional error component is due to the fact that the vehicle navigation system may contain accumulated errors of approximately 10 m.

[1]The vehicle is performing ded-reckoning based on acoustic Doppler data with periodic navigation updates based on data from a long baseline (LBL) acoustic buoy transponder system. The position updates to the ded-reckoned position based on the LBL data are referred to as navigation fixes.

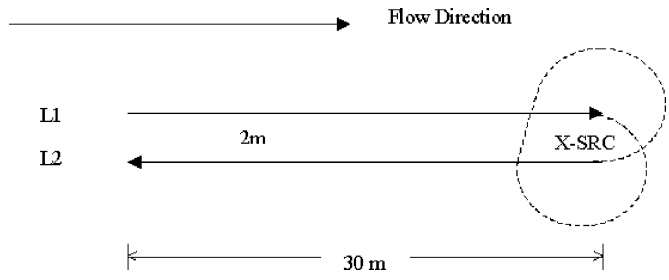

Fig. 4. Illustration of the FLYBY maneuver.

Note that the chemical source is on the bottom and that the AUV drives at a nonzero altitude above the bottom (altitude of 1.5 to 2.0 m is commanded). Therefore, the chemical plume does not rise to the altitude of the AUV, which is necessary for the AUV to detect the chemical, until the chemical has traveled some distance from the source in the direction of the flow. This distance is flow-dependent and is not known. Therefore, the declared source location is expected to have an error component, relative to the true source location, that is in the direction of the flow.

C. Behavior Coordination

Behaviors 1 through 5, described in Section III-A, are switched based on Boolean logic as indicated in the pseudocode of each behavior and Fig. 2. Only one of Behaviors 1 through 5 was active at any given time. Behavior 6, when active, can modify the command of any of the other behaviors.

D. Postdeclaration Behaviors

After the source location has been declared, it is sometimes useful to perform special maneuvers relative to the declared source location. These special maneuvers are designed to acquire additional sensor data, possible from auxiliary sensors.

1) FLYBY: As described in the section describing the declaration decision, the declared source location is expected to be several meters downflow from the true source location. The FLYBY maneuver was designed to verify this fact. This maneuver was only useful during tests where an underwater video camera was focused on the chemical source.

The FLYBY maneuver is depicted in Fig. 4 where "X" marks the declared source location. The AUV is commanded to drive to a starting point 30 m upflow from the declared source location and to arrive at that point with a heading in the downflow direction. The AUV is then commanded to follow a line between that starting location and the declared source location. After completing that line, the AUV reverses its direction and follows a line from the declared source location to an end point 30 m upflow from the declared source location. The two lines are separated by 2 m in the crossflow direction.

When an underwater camera is focused on the source, this maneuver should cause the AUV to be captured on video as it passes the source either in the upflow or downflow direction. Note that no other behavior commands the AUV to drive in the downflow direction. Therefore, this behavior is distinct and easily observable on the video image [18].

2) STAMP: The AUV has a sidescan sonar mounted on it. The sidescan sonar imagery is useful for determining ground truth source location in the same coordinate system as the CPT algorithm. To obtain good quality sidescan imagery of the source, the AUV must be near (within 30 m lateral to the AUV, but not directly over) the source and the AUV attitude should be constant. The STAMP maneuver shown in Fig. 5 was designed by the Navy to acquire useful sidescan imagery. The symbol "X" indicates the declared source location. Lines L5 – L8 should be parallel to the flow. Lines L1 – L4 should be perpendicular to the flow. Lines L2 and L3 should be separated by 40 m. Lines L6 and L7 should be separated by 40 m. The lines were traced in the order L1, L3, L2, L4, L5, L7, L6, L8 to ensure that sequential lines are spaced wide enough apart to be achievable by the AUV. After the AUV was returned to the dock, the sidescan imagery acquired during this maneuver was analyzed by Navy personnel who determined the 'ground truth' source location for comparison with the location declared by the CPT algorithms.

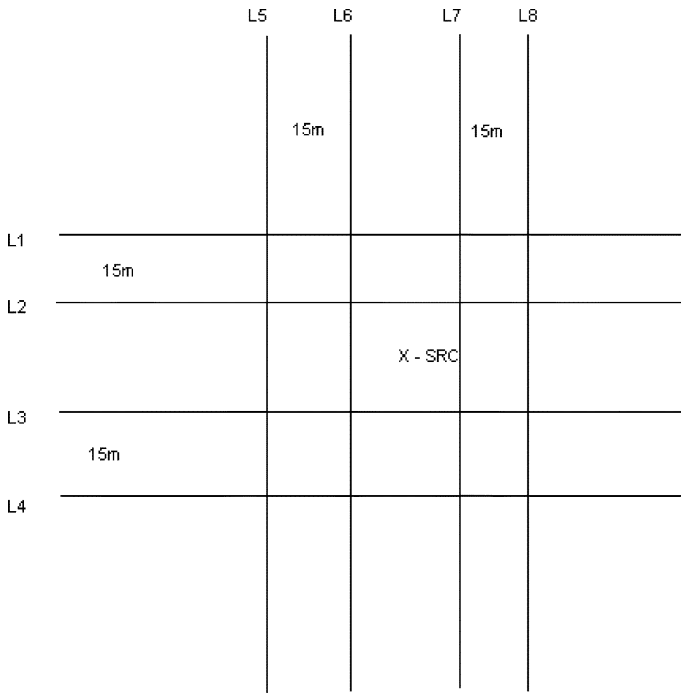

Fig. 5. Desired lines to be followed for the STAMP maneuver, assuming that the flow is from top to bottom.

TABLE IV
PARAMETER SETTINGS FOR CPT STRATEGY FOR THE APRIL 2003 SCI AND JUNE 2003 DUCK EXPERIMENTS

Symbol	Behavior	Value
λ	Track-In	5.0 s
β	Track-In	20 deg
L_u	Track_Out	18.0 m
L_c	Track_Out	18.0 m
N_re	Reacquire	2
K	Guidance	5.0
R	Guidance	10.0 m

IV. FIELD TESTS

Two variations of CPT algorithms were tested in four different sets of experiments. A first CPT algorithm, described with experimental results in [18], was tested at San Clemente Island (SCI), CA, in September 2002 and at SCI in November

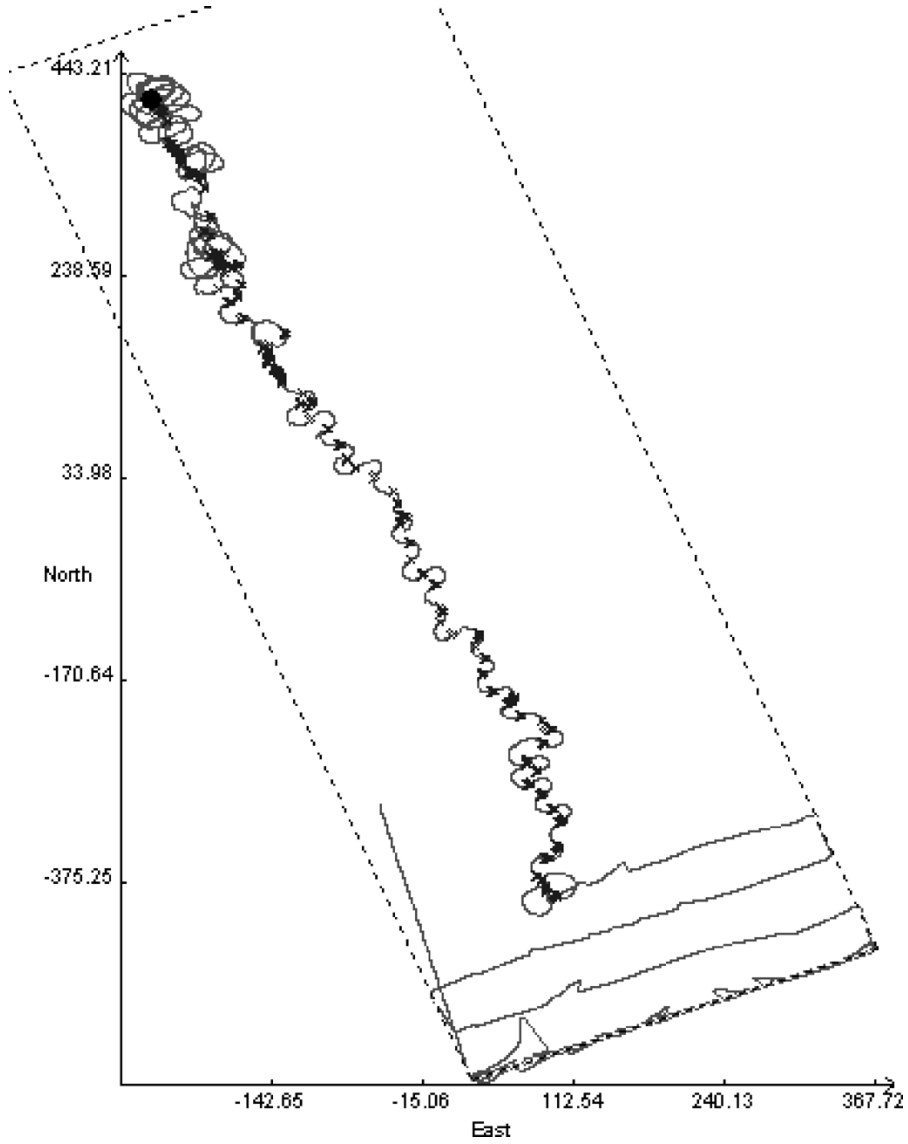

Fig. 6. Trajectory and chemical detection points. The dashed rectangle is the operating area boundary. The solid curve is the AUV trajectory. Each x marks the location of a chemical detection. The black dot at $(\mathrm{N}, \mathrm{E}) = (414, -242)$ m marks the declared source location.

2002. Based on the results of those tests, the Find, Reacquire, and Source Declaration behaviors were revised and the post-declaration maneuvers were added. The revised CPT strategy described herein using the parameters shown in Table IV was experimentally tested at SCI in April 2003 and at Duck, NC in June 2003. The April 2003 experiments successfully declared the source location on 7 of 8 experiments. The experiments included ground truth confirmation of declared source locations via sidescan sonar and several Flyby maneuvers captured on video. In fact, one Flyby maneuver resulted in a collision with the source that was caught on video. The algorithms and field test results described herein, unless otherwise noted, are from the June 2003 experiments in Duck, NC.

Two types of missions were of interest during this set of experiments. The first mission type, labeled ST, contained a single chemical source in the OpArea. The ST mission was intended to find the plume, to trace a plume over a long distance, and to declare the source location. This mission demonstrates detection and tracing of plumes over long distances. The second mission type, labeled MT, may contain a few chemical sources in the OpArea. In an MT mission, the OpArea will be divided into subregions. The AUV will search each subregion for chemical until one of three events occurs. First, the search within a subregion may timeout. In this case, the subregions is declared source free and the AUV moves on to the next subregion. Second, the AUV may detect chemical and declare a source location within the region. It will then move on to the next subregion. Third, the AUV may trace chemical to the upflow edge of the region. In this case, a source will be declared at the intersection of the plume with the upflow edge of the subregion and the AUV will move on to the next subregion. When the declared source locations are analyzed at the end of an experiment it is up to the test director to decide whether source locations at the edge of a subregion are due to sources near that location or the result of plumes generated by sources in the adjacent region.

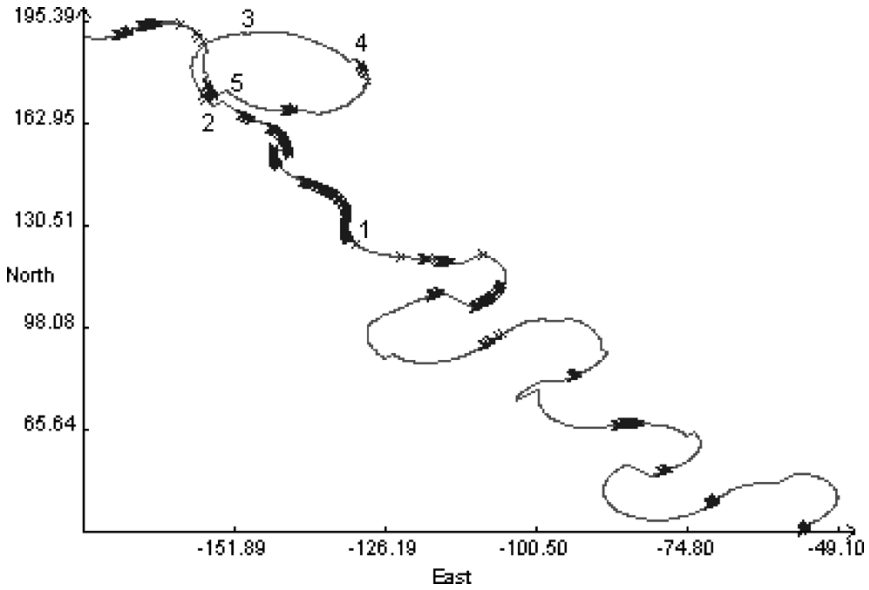

Fig. 7. Magnified view of Fig. 6 for t in [2400,2600] s.

The AUV for these tests was the Albacore REMUS owned by SPAWAR in San Diego, CA. The REMUS was modified to contain a PC104 computer to run the AMP CPT algorithms. The AMP computer received sensor data from the REMUS computer via serial port, processed the sensor data, and output heading, speed, and depth/altitude commands to the REMUS computer via the same serial port.

Up and down looking acoustic Doppler current profilers (ADCP) were onboard the REMUS. Algorithms described in Appendix B used the ADCP data to compute the fluid flow. The AUV also had a CTD mounted onboard, but it was not used due to its slow response time. Also, the AUV used long baseline transducers with acoustic buoys in conjunction with ded-reckoning based on ADCP data to determine onboard AUV position. Finally, a fluorometer was mounted near the nose of the AUV. The fluorometer was capable of detecting Rhodamine dye from a source that was used to create the plume for these experiments. The fluorometer sample rate was 10 Hz.

Figs. 6–9 show the trajectory (solid line), chemical detection locations (x's), and declared source location (black dot) for three missions performed at Duck, NC, in June 2003. The boundary of the OpArea is indicated by the dashed line. These experiments were performed in 4–8 m of water. The bottom was gradually sloping from the coast. The coast is approximately 400 m to the left of boundary of the OpArea in all figures in this section. During all experiments included herein, the water column consisted of a top layer flowing northerly with a speed near 20–25 cm/s and a bottom layer flowing southerly with a speed greater than 10 cm/s. The depth of the boundary layer between these two flow regimes changed with location and time.

Figs. 6–9 use a coordinate system that is defined in the north and east directions relative to the center of the OpArea. The OpArea is the same for Figs. 8 and 9, but is different for Fig. 6. Four chemical sources were available. Each mission has a different set of sources turned on.

Fig. 6 shows the trajectory, chemical detection locations, and declared source location for an ST mission. For this mission, the OpArea was 367×1094 m (greater than 60 football fields). During this experiment, the flow calculated on the AMP varied in magnitude between 10 and 15 cm/s and in direction between 110 and 147 deg. For this experiment, the commanded speed was 2 m/s and the typical AUV altitude was 2.0 m. The actual altitude varies by plus or minus 0.7 m relative to the commanded altitude. To challenge the CPT algorithm, we wanted the first chemical detection to occur as far as possible from the chemical source. Therefore, the source is located near the upflow edge of the OpArea and the AUV starts the mission near the downflow edge of the box. The AMP CPT algorithms start as soon as chemical is detected. This mission tracks the chemical plume for 976 m between the first detection point and the declared source location. The source is declared at 36n11.028, 75w44.620. The ground truth source location is 36n11.035, 75w44.621 as found from sidescan data acquired during a STAMP maneuver centered on the declared source location. The declared source location is 13 m south and 2 m east of the sidescan sonar location. Note that this error is predominantly in the direction of the flow, as expected.

Fig. 7 shows a magnified view of Fig. 6 for t in [2400,2600] s. At 2400 s, the AUV is near the lower right of Fig. 7. During this timeframe, the AUV makes up-plume progress from the lower right toward the upper left. Prior to the time indicated by the numeral 1, the BBP is switching between Track-In and Track-Out. Between the times indicated by 1 and 2, the detections are near enough in time that the BBP is able to drive up the plume using Track-In. Notice that the cross-plume maneuvering is much smaller using only the Track-In behavior. Between the times indicated by the numerals 2 and 3, the Track-Out behavior fails to redetect the chemical so that the BBP switches to Reacquire. As the AUV maneuvers toward the first line of the Bowtie, chemical is detected near the location indicated by the numeral 4 and the BBP switches to Track-In.

The expanded scale of Fig. 7 makes it easier to notice the occurrence of navigation fixes. A navigation fix occurs when the position determined from signal return times to transpon-

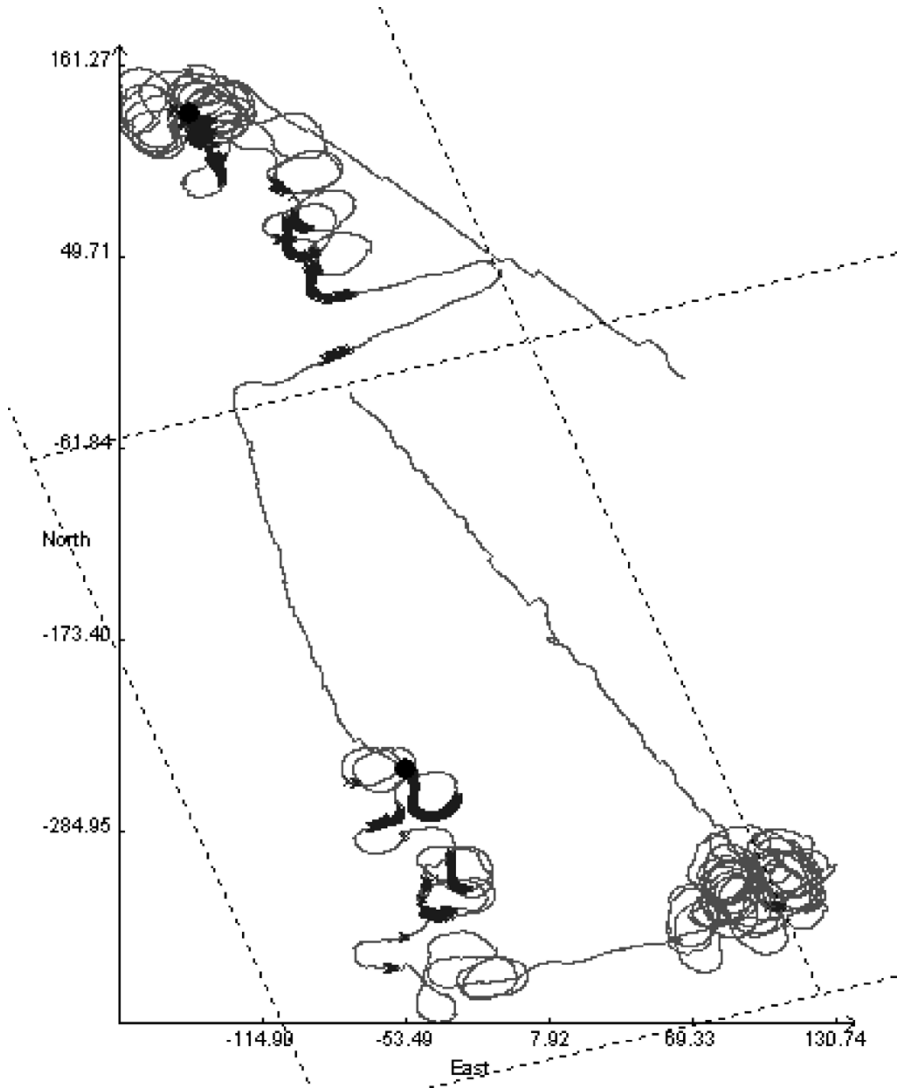

Fig. 8. Trajectory and chemical detection points. The dashed rectangle is the operating area. The solid curve is the AUV trajectory. Each x marks the location of a chemical detection. The black dots mark the declared source location.

ders disagrees significantly with the position computed based on ded-reckoning. In this case, the ded-reckoned solution is updated based on the position determined using the transponders. These updates are easily noticeable as the discontinuous changes in the otherwise smooth AUV trajectory. Since the BBP is implemented using the guidance Go to Point, Go to Point with Heading, and Follow Line commands and the guidance system implements these commands using feedback, the BBP is robust to navigation errors.

Fig. 8 shows the trajectory, chemical detection locations, and declared source locations for an MT mission. The four subregions are outlined by dashed lines in Fig. 8. During this experiment, the flow calculated on the AMP varied in magnitude between 17 and 22 cm/s and in direction between 160 and 170 deg. For this experiment, the commanded speed was 2 m/s and the commanded (and typical) altitude was 1.5 m. Early in the mission, chemical is detected near the southeast corner of the first (southwest) region. The AUV operates near that detection point until the list of lost detection points is empty and then reverts to the find plume behavior. Note that this maneuvering is correct, since chemical is detected, but there are not enough repeated detections over a series of maneuvers to make a source declaration. Later, chemical is detected and tracked a distance of 164 m to a source that is declared at 36n10.825, 75w44.552. Sidescan sonar data confirmed the source at 36n10.826, 75w44.543. The error between these locations is 14 m in the crossflow direction. After declaring the source in the first region, AMP drove the AUV to the second (northwest) region and restarted the CPT algorithm. Note that the AMP CPT algorithm is designed to ignore chemical detections while in transit using the GoTo command. Therefore, CPT does not initiate in the second region (northwest) until the vehicle reaches the east boundary of that region. In the northwest region, chemical is detected and tracked a distance of 126 m to a source that is declared at 36n11.032, 75w44.614. Sidescan sonar data confirmed the source at 36n11.036, 75w44.622. The error between these locations is 14 m in the crossflow direction. Note that this declared source is the same as that from the mission shown in Fig. 6 and that the latitude and longitude of the declared and sidescan sonar source locations closely match with those for

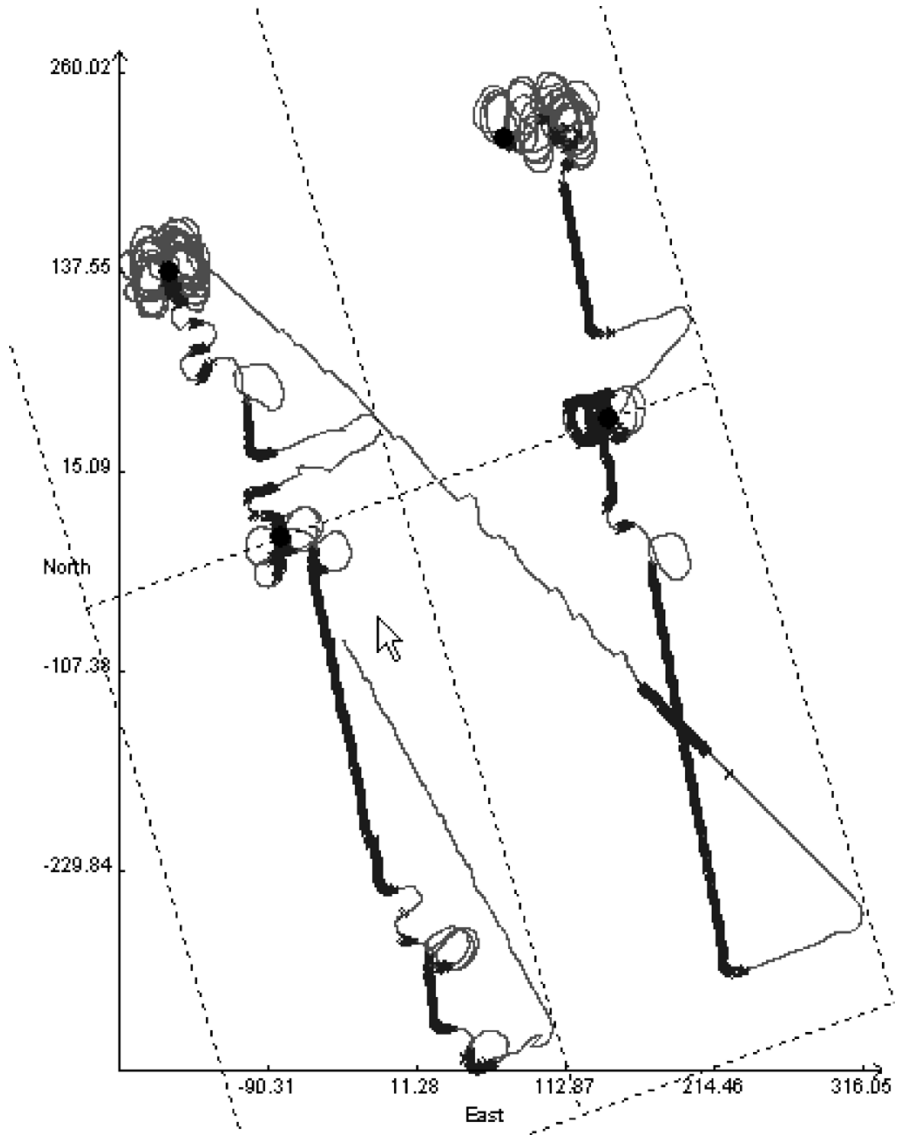

Fig. 9. Trajectory and chemical detection points. The dashed rectangle is the operating area. The solid curve is the AUV trajectory. Each x marks the location of a chemical detection. The black dots mark the declared source location.

Fig. 6. The N,E coordinates do not match, since the origin of the OpAreas are not the same. After declaring the source in the northwest region, AMP drove the AUV to the southeast region. Prior to AMP starting the Find behavior in third region, the test director aborted the mission, as it was too late in the day to safely continue.

Fig. 9 shows the trajectory, chemical detection locations, and declared source locations for an MT mission. The four subregions are outlined by dashed lines in Fig. 9. During this experiment, the flow calculated on the AMP varied in magnitude between 20 and 30 cm/s and in direction between 160 and 175 deg. For this experiment, the commanded speed was 2 m/s and the commanded (and typical) altitude was 1.5 m. The southwest region is explored first. Chemical is detected and tracked for 351 m to the boundary between the southwest and northwest regions. The source for the first region is declared (correctly) at this boundary. Then, AMP drives the AUV to the northwest region. In the northwest region, the plume is tracked for an additional 180 m with a source declared at 36n11.034, 75w44.621. Sidescan sonar data confirmed the source at 36n11.037, 75w44.622. The error between these locations is 6 m in the downflow direction. Note that this declared source is the same as that (for the same quadrant) from the missions shown in Figs. 6 and 8. Note that the latitude and longitude of the declared and sonar source locations match closely between these figures.

After declaring the source in the northwest region, AMP drove the AUV to the southeast region and restarted the CPT algorithm. During the transition from the northwest region to the southeast region using the GoTo command, chemical detections are ignored. In the southwest region, chemical is detected and tracked a distance of 351 m to a source that is declared (correctly) on the boundary between the southeast and northeast regions. Then AMP drives the AUV to the northeast region. In the northeast region, the plume is tracked for an additional 185 m with the source declared at 36n11.079, 75w44.468. Sidescan sonar data confirmed the source at 36n11.087, 75w44.450. The error between these locations is

31 m in the crossflow direction. This crossflow error is clearly visible in the northeast region of Fig. 9. This crossflow error is an artifact of a navigation fix that occurred prior to the declaration and the declaration logic that only accounted for position differences in the direction of the flow. This will be fixed in future versions of the algorithm.

Note that in spite of the exact same strategy and parameters being used in all runs, the nature of the trajectories shown in Figs. 6, 8, and 9 during the plume tracing phase look different. Therefore, the differences in experimental conditions deserve comment. First, the mission shown in Fig. 6 was one of the first trials at Duck, NC. Due to the fact that we were operating in an unknown environment, the REMUS minimum safe operating altitude for that mission was defined to be 2.0 m. For the missions corresponding to Figs. 8 and 9, the REMUS minimum safe operating altitude for that mission was defined to be 1.5 m. Analysis of the log files show that plume tracing for the mission of Fig. 6 frequently used the Track-Out behavior, which relies on large magnitude turns designed to cross the plume. Fig. 6 clearly shows this behavior. Plume tracing for the mission shown in Fig. 9 primarily used the Track-In behavior, since its small angle counterturning caused the AUV to drive up the main body of the plume. The difference in commanded altitudes could be the major reason for this difference, if the 2 m altitude of Fig. 6 only allowed the AUV to intermittently contact the top of the plume. Note also that in Fig. 9, as the AUV approaches the source, it must use the Track-Out behavior more frequently, because near the source the plume is still at a lower altitude.

The source declaration and plume tracking that occurred in the southwest quadrant of Fig. 8 is also interesting. This chemical source near the center of the southwest quadreant was turned off during this experiment, but had developed a leak that was not discovered until the AMP tracked its plume and declared the source location. After this, divers were dispatched and verified the fact. Since that plume was from a leak, its plume may have been at lower concentration and more intermittent than the other plumes that were created by pumped sources. Nonetheless, the plume was traced and the chemical source was accurately declared. Note that the trajectory for this plume trace exhibits several Track-Out and Reacquire maneuvers.

V. Discussion

It is important that the commanded trajectories be within the maneuverability and instrumentation limits of the AUV. For example, the AUV computes its position by a combination of dedreckoning (i.e., integration of speed after rotation from vehicle to navigation frame) and navigation updates based on positions calculated from transponder signal return times. The required rotation matrix utilizes a yaw variable compute based on the integration of a yaw rate gyro. If the yaw rate gyro were to saturate, the yaw rate, yaw angle, and computed position would all subsequently be wrong. To ensure that the heading commands issued from the BBP to the guidance system were reasonable, the BBP heading was filtered prior to being sent to the guidance system. This command filter imposed a bandwidth of 5.0 rad/s and a rate limit of 10 deg/s on the BBP output heading command. Careful analysis of mission data shows that large ($> 10\,\mathrm{m}$) position fixes are rare during the time that the AMP is driving the AUV.

The values of the parameters of the CPT strategy are summarized in Table IV. The motivation for these values and the effect of changes to the λ and β values are discussed at length in [15]. That paper describes various simulations studies that motivated the counterturning approach implemented in the Track-In behavior. If β is increased, then the counterturns have a larger cross flow component. The tradeoff is that the larger crossflow component increases the probability that the AUV exits the plume from the expected edge (i.e., the variable LHS is more likely to be correct), but increases the length of the trajectory to get to the source. The variable λ should be larger than the intermittent chemical detection gaps while in the plume; however, the plume intermittency is dependent on characteristics of the flow and turbulence that are not known. Typical "in the plume" interpulse durations are less than 1 s [13]. As λ is increased, if chemical is not detected, then the distance that the AUV moves from the last detection point is increased. As long as this distance is less than $\mathrm{L_u}$, then no backtracking is required. For these experiments, $\nu_\mathrm{c} = 2.0\,\mathrm{m/s}$. Therefore, for $\lambda = 5\,\mathrm{s}$, the distance traveled is 10 m which is less than $\mathrm{L_u}$. The value of $\mathrm{L_c}$ was selected to ensure that, even with navigation errors ($< 10\,\mathrm{m}$ nominally) and with the GoTo guidance command being satisfied when the AUV was within 10 m of the destination, the AUV would cross a line extending upflow from the last detection point. The value of $\mathrm{N\_re}$ was set to 2. Increasing $\mathrm{N\_re}$ causes the AUV to spend additional time searching upflow from each point on the lost_pnts list. This additional time is detrimental when the BowTie's are upflow from a false-alarm detection point (see the lower right detection point of Fig. 8). The values of K and R are dependent on the dynamic capabilities of the AUV. These values were determined in simulation and evaluated onboard the AUV prior to the CPT experiments described herein.

The CPT strategy described herein with the parameters of Table IV was evaluated extensively in simulation and used in experiments at SCI CA and Duck, NC. The experimental conditions are distinctly different at SCI CA and Duck, NC. Due to kelp, the available maximum OpArea at SCI is restricted to 100×300 m. At Duck, the OpArea was select to be 360×1000 m. At SCI, the water depth increases rapidly from 12 to 24 m across the 100 m width of the OpArea. At Duck, the water depth increases from 4 to 8 across the 367 m width of the OpArea. At SCI, the bottom boundary layer was wide enough that we did not experience any significant issues with it. At Duck, due to the shallow water and the AUV cruising near 1.5 to 2 m altitude, it was difficult to maintain the AUV mounted chemical sensor and upward looking ADCP effective sensing location both in the bottom boundary layer. The SCI test location was on the side of island closest to the CA coast; therefore, the test location was relatively isolated from waves. The Duck test location is directly exposed to the Atlantic ocean and had significant waves. Finally, the SCI test location typically had flow magnitudes less than 10 cm/s with direction reversals possible after a few hours. The Duck test location typically had flow magnitudes greater than 20 cm/s with relatively constant (i.e., nonreversing) direction for greater than 6 h. In addition, the top layer flow at Duck was in the opposite direction with

a flow magnitude near 25 cm/s. The fact that the same CPT algorithm with the same parameters settings performed equally well in both of these experiments demonstrates a high level of robustness to environmental conditions.

Note also, that the definition of a chemical detection implicitly contains two parameters: the detection threshold and the number of above threshold readings required to declare a detection. For all variations of CPT strategies that we performed during this three year program, the definition of a chemical detection was a concentration $\mathrm{c(t)} > 4\%$ of full scale (i.e., 0.2 V). This value was determined by analysis of chemical sensor data from the AUV operating in San Diego Bay (August 2002) in the absence of the chemical. In this scenario, the sensor readings were pure noise, but never surpassed 0.2 V. Therefore, we selected the threshold such that the probability of false alarm readings was extremely low. Therefore, any single sensor reading above threshold was registered as a chemical detection. The number of above threshold readings required to register a detection could be increased. This would decrease the probability of false alarms, but increase the probability of missed detections. Note that the detections in the lower right of Fig. 8 are not false alarms. There are actually several sequential detections at that point. This is apparently chemical left in the water from a previous experiment. The BBP does spend significant time near these detections before working through the lost_pnts list; however, the BBP does ultimately declare the correct source location for that region.

An important question is whether AMP strategies (with fixed parameters) are more accurate, robust, or efficient than preplanned strategies. In fact it was the lack of accuracy, robustness, and efficiency of preplanned strategies for this mission that motivated the Navy to pursue this research project. The typical preplanned mission for this application is illustrated by the dashed line (column search) shown in Fig. 1. The legs of the search are preplanned to be perpendicular to the expected flow direction. If the region dimensions are L (parallel to the flow) by W (perpendicular to the flow) and the desired search resolution is d, then $N = ceil(L/d)$ legs of length W are required, where 'ceil' returns the smallest integer greater than its argument. Therefore, the nominal search length is

$$\mathrm{NW} + (\mathrm{N}-1)\pi\left(\frac{\mathrm{d}}{2}\right).$$

Note that this length is proportional to the *area* of the region to be searched. Note that it does not matter where the source is in the region, as the entire preplanned mission will always execute. The length of the AMP CPT trajectory is proportional to the distance from the first point of chemical detection to the declared source location. However, robustness and accuracy of source declaration are the more important motivating factors. The accuracy of the preplanned mission is expected to be d, but this is not certain because the actual flow may not align with the expected flow. In addition, many factors can cause any particular plume crossing to fail to detect the plume. This is particularly true in the vicinity of the source, where the AUV may pass over the plume.

We have intentionally phrased the previous paragraph in terms of generic AMP strategies instead of the specific strategy that we used in these experiments. With the current AMP strategy and experimental results in mind, many alternative and possibly improved AMP strategies could be proposed. In fact, one of the goals of any experiment should be to identify areas for future improvements. Therefore, it is important to consider what lessons were learned in these experiments. First, care should be taken to ensure that the ADCP flow data corresponds to the flow layer containing the plume; however, this is not straightforward. For the Duck, NC test location, the water is 4–8 m deep. The bottom boundary layer depth varied with time. The minimum safe AUV operating altitude was 1.5 m and the ADCP has an approximately 0.75 m deadzone prior to its measurement being accurate. Therefore, there were runs for which the upward looking ADCP was measuring the flow in the top layer instead of the bottom layer. Detecting and accommodating such events would require significant advancements for the planner and possible a conductivity, temperature, and depth (CTD) sensor with a fast response time. Second, some of the declared source locations had unexpected error in the crossflow direction, which was unexpected. We believe that this error component is due to navigation fixes that occurred near the time of declaration and by the declaration logic that ignored separation in the crossflow direction. The source declaration logic described herein was based only on the along flow separation of points at which the plume was lost. The crossflow separation was ignored in the declaration process to decrease the time required to make a declaration. Accounting for crossflow separation in the declaration logic would improve the accuracy of the declaration and is straightforward to implement in the future. Third, the current AMP strategy used the chemical sensor in a Boolean mode even though the sensor did provide an analog reading. It is often suggested that the analog concentration could provide a useful indicator of the distance to the source; however, there are a few difficulties in this approach. First, the chemical source concentration would be unknown in a real application. Second, the rate of decay of the peak concentration reading as a function of the distance from the source is flow dependent and not known. Third, maximum sensed concentration along any transect is not necessarily the maximum concentration in the vicinity of that transect. Alternative, the analog sensor reading could have utility in experiments where multiple sources might generate overlapping plumes. In that scenario, a significant decrease in the maximum sensed chemical while moving upflow might indicate that a source has just been passed by while the AUV is still in the plume of another source. Such strategies were not required for this project.

It is also interesting to consider adaptation of the AMP strategy parameters based on distance from the source. For example, it might be more efficient to decrease $\mathrm{L_u}$ and $\mathrm{L_c}$ as the AUV gets nearer to the source. The difficulty in implementing such ideas is in evaluating the distance to the source when the source location is unknown. Early in the program, we hoped that the width of plume transects would be a useful indicator of the distance to the source. This proved futile for a variety of reasons: plume meander results in AUV transects being at different angles relative to the plume centerline; a variety of factors result in AUV transects being at different altitudes

relative to the plume centerline altitude; and, the instantaneous plume width at a fixed distance from the source varies widely. Similarly, sensed chemical concentration is not a useful indicator of distance to the source since the source concentration is unknown and the sensed concentration at a fixed distance from the source varies widely.

VI. Summary and Conclusion

This paper has presented adaptive mission planning algorithms and experimental results for the first demonstration of chemical plume tracing by an AUV. The experiments occurred in a near shore ocean environment. Plume tracing was demonstrated over distances of 975 m with average source declaration accuracy of approximately 13 m.

Appendix

The following sections provide short descriptions of other essential algorithms used in these missions.

A. Guidance

This appendix describes the implementation of the three guidance modes that were used to implement the planner behaviors. In any of these modes, the guidance function will output depth/altitude and earth relative velocity (geographic heading and speed) commands. For accurate implementation of the desired trajectory, these commands should be compensated for the flow vector to produce water relative speed $\mathrm{u_c}$ and ground relative yaw commands $\psi_{\mathrm{g}}^{\mathrm{t}}$

$$\begin{aligned}\mathrm{V_f} &= \mathrm{V_g} - F_{\mathrm{g}}\\ \psi_{\mathrm{g}}^{\mathrm{t}} &= \mathrm{atan2}[(\mathrm{v_f}, \mathrm{u_f})^{\mathrm{t}}]\\ u_{\mathrm{c}} &= ||\mathrm{V_f}||\end{aligned}$$

where $\mathrm{V_f} = (\mathrm{u_f}, \mathrm{v_f}, \mathrm{w_f})$ is the water relative AUV velocity, $\mathrm{V_g}$ is the ground relative AUV velocity, and $\mathrm{F_g}$ is the ground relative flow vector (see Appendix B). A superscript indicates a coordinate frame: 't' for geodetic tangent frame or 'b' for body frame. The components of vector $\mathrm{V_f^t}$ are $(\mathrm{u_f}, \mathrm{v_f}, \mathrm{w_f})^{\mathrm{t}}$.

1) Go-To: This function is used to drive the AUV from its present location to a destination, without regard to the heading at the destination location. Let $(x(t), y(t))$ be the current AUV position and (x_d, y_d) be the destination location. The commanded geographic heading is

$$\psi_{\mathrm{c}}(t) = \arctan(y(t) - y_d, x(t) - x_d).$$

When the AUV is within a radius R of the destination location, it is considered to have arrived at the destination location and the planner will exit from the Go-To mode.

2) Follow Line: During CPT, sometimes the AUV needs to track a straight line. Given two locations (x_s, y_s) and (x_d, y_d) in the operation area, a line segment L_{sd} is defined that starts from point (x_s, y_s) and ends at point (x_d, y_d). The follow line mode, depicted in Fig. 10, will generate a sequence of heading and speed commands which will make the AUV trajectory follow the line L_{sd}. The first step of the follow line mode is to drive the AUV to the start point (x_s, y_s) while ensuring that the AUV

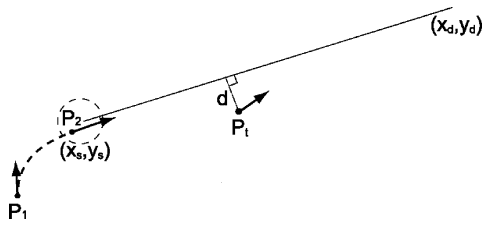

Fig. 10. Definition of variables for the follow line mode.

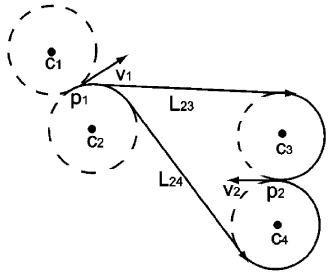

Fig. 11. Depiction of the go to point with heading mode.

heading ψ upon arrival at the start of the line is about the same as the line orientation angle

$$\alpha_{sd} = \arctan(y_d - y_s, x_d - x_s).$$

The 'Go to Point with Heading' mode is discussed in the following subsection.

When the AUV is within radius R of the start point and within heading angle θ of α_{sd}, the AUV will begin to follow the line. Define the distance d between the AUV position $\mathrm{P_t} = (x(t), y(t))$ and the line to be positive when the AUV is on the left side of the line L_{sd} (when looking from start point (x_s, y_s) to the goal point (x_d, y_d) and negative when the AUV is on the right side of the line. The corresponding heading command is

$$\psi_{\mathrm{c}}(t) = \begin{cases} \alpha_{sd} + K \times d & d < d_1 \\ \alpha_{sd} + \mathrm{sign}(d) \times 45 & d \geq d_1 \end{cases}$$

where K is a predefined gain, $d_1 = 45/\mathrm{K}$, and the $sign$ function is defined as

$$\mathrm{sign}(x) = \begin{cases} 1 & x \geq 0 \\ -1 & x < 0 \end{cases}.$$

3) Go to Point With Heading: The goal of this mode is to drive the AUV from a start position and orientation angle to a destination position and orientation angle with the constraint that desired trajectory cannot violate a prespecified minimum turning circle. This guidance mode is significantly more complicated than it first appears. It was proved by Dubins [40] that this trajectory consists of exactly three path segments. It is either a sequence of CCC or CSC, where C (circle) is an arc of minimal turning radius R_m and S (straight line) is a line segment. In our application, we only use the CSC trajectory. Even though the CSC trajectory sometimes is not the shortest path, it is easy to generate this trajectory, thereby saving computational resources.

Fig. 11 shows an example of Go to Point With Heading. The AUV starts from position p_1 with orientation angle θ_1 and

should go to position p_2 with orientation angle θ_2. Here we use two unit vectors V_1 and V_2 to represent the start and destination positions and orientation angles. First, we generate four circles C_1, C_2, C_3, C_4, whose radii are the minimal allowed turning radius R_m. The first two circles C_1, C_2 are tangent to V_1 at p_1, C_3, C_4, are tangent to V_2 at p_2. Note that arcs C_1, C_4 are counterclockwise and C_2, C_3 are clockwise. Second, we generate four line segments L_{ij}, where $i = 1,2$ and $j = 3,4$ (only showing two lines in Fig. 11). Line L_{ij} connects C_i to C_j in a continuous fashion. Now, we have four possible candidate paths, namely, $C_1L_{13}C_3; C_1L_{14}C_4; C_2L_{23}C_3; C_2L_{24}C_4$. Third, we calculate the length for each of the four candidate paths and select the shortest path as the trajectory for the AUV.

B. Flow Computations

The REMUS has upward and downward looking acoustic Doppler current profilers (ADCPs). Each ADCP measured fluid relative velocity is averaged over a bin between 0.75 and 1.25 m above or below the AUV. Since during CPT the AUV operates in a bottom following mode at low altitudes (1.5–2.5 m), the data from the downward looking ADCP frequently is not valid and is therefore not used. Each ADCP provides data to the REMUS computer, which sends the AUV altitude and heading, the AUV ground relative velocity in body frame $\mathrm{v_g^b} = (\mathrm{u_g}, \mathrm{v_g}, \mathrm{w_g})^{\mathrm{b}}$ and the AUV fluid relative velocity in body frame $\mathrm{v_f^b} = (\mathrm{u_f}, \mathrm{v_f}, \mathrm{w_f})^{\mathrm{b}}$ to the AMP every 1.0 seconds. The messages alternate between the upward and downward looking ADCP so that the effective per sensor sample period is 2.0 s.

ADCP data received by AMP while in a normal operating mode is processed when all four of the following conditions are met: $(\|\mathrm{v_g^b}\|_2 > 0.4)$ and $(\|\mathrm{v_f^b}\|_2 > 0.003)$ and $(\mathrm{depth} > 1\ \mathrm{m})$ and $(\mathrm{altitude} > 1\ \mathrm{m})$. When these conditions are met, the earth relative flow in tangent frame $\mathrm{f_g^t}$ is calculated as

$$\mathrm{f_g^t} = \mathrm{R_{b2t}}(\mathrm{v_g^b} - \mathrm{v_f^b})$$

where $\mathrm{R_{b2t}}$ is the rotation matrix to transform from body frame to tangent frame. A circular buffer of 100 past $\mathrm{f_g^t}$ vectors is saved. The average of the elements of this buffer is denoted as $\mathrm{F_g^t}$. The present calculated flow vector $\mathrm{f_g^t}$ replaces the oldest element of this buffer of flow data when the present flow vector satisfied the following conditions: $(\|\mathrm{f_g^t}\|_2 < 0.35)$ and $(\|\mathrm{f_g^t} - \mathrm{F_g^t}\|_1 < 0.4)$. The buffer average $\mathrm{F_g^t}$ is used to compute the flow direction and flow magnitude that is used in the AMP CPT algorithms. Due to the 0.5-Hz sampling of the upward looking ADCP and the 100-sample average, the computed flow requires several tens of seconds to change significantly. The 100-sample average was require to accommodate the per sample noise in the computed flow.

ACKNOWLEDGMENT

R. Cardé and J. Murlis were key collaborators while developing the theory for CPT under the ONR/DARPA CPT program. R. Arrieta, J. Deschamps, V. Djapic, A. Dreiling, B. Granger, P. Holland, G. Hong, B. Morris, P. Selwyn, K. Vierra, and the N. Divers were key collaborators during the experimental phase of this effort. Arete Associates provided a graphic that was edited to produced Fig. 1. R. Stokey and G. Packard at WHOI were instrumental in getting the AMP on and communicating with the REMUS. The speed, heading, altitude control, and position estimation algorithms were all the standard algorithms developed by WHOI for REMUS.

REFERENCES

[1] D. B. Dusenbery, *Sensory Ecology: How Organizms Acquire and Respond to Information*. New York: W.H. Freeman, 1992.
[2] N. J. Vickers, "Mechanisms of animal navigation in odor plumes," *Biol. Bull.*, vol. 198, pp. 203–212, 2000.
[3] R. K. Zimmer and C. A. Butman, "Chemical signaling processes in the marine environment," *Biol. Bull.*, vol. 198, pp. 168–187, 2000.
[4] A. D. Hassler and A. T. Scholz, *Olfactory Imprinting and Homing in Salmon*. New York: Springer-Verlag, 1983.
[5] G. A. Nevitt, "Olfactory foraging by antartic proellariiform seabirds: Life at high Reynolds numbers," *Biol. Bull.*, vol. 198, pp. 245–253, Apr. 2000.
[6] J. Basil, "Lobster orientation in turbulent odor plumes: Simultaneous measurements of tracking behavior and temporal odor patterns," *Biol. Bull.*, vol. 187, pp. 272–273, 1994.
[7] D. V. Devine and J. Atema, "Function of chemoreceptor organs in spatial orientation of the lobster, Homarus ameri-canus: Differences and overlap," *Biol. Bull.*, vol. 163, pp. 144–153, 1982.
[8] M. J. Wiesburg and R. K. Zimmer-Faust, "Odor plumes and how blue crabs use them in finding prey," *J. Exper. Biol.*, vol. 197, pp. 349–375, 1994.
[9] M. J. Weissburg and D. B. Dusenbery, "Behavioral observations and computer simulations of blue crab movement to a chemical source in a controlled turbulent flow," *J. Exper. Biol.*, vol. 205, no. 21, pp. 3387–3398, 2002.
[10] R. T. Cardé, "Odour plumes and odour-mediated flight in insects. In olfaction in mosquito-host interactions," in *CIBA Found. Symp.*, vol. 200, 1996, pp. 54–70.
[11] R. T. Cardé and A. Mafra-Neto, "Mechanisms of flight of male moths to pheromone," in *Insect Pheromone Research.New Directions*, R. T. Cardé and A. K. Minks, Eds. New York: Chapman and Hall, 1996, pp. 275–290.
[12] J. S. Elkinton, C. Schal, T. Ono, and R. T. Cardé, "Pheromone puff trajectory and upwind flight of male gypsy moths in a forest," *Phys. Entomol.*, vol. 12, pp. 399–406, 1987.
[13] C. D. Jones, "On the structure of instantaneous plumes in the atmosphere," *J. Hazard. Mater.*, vol. 7, pp. 87–112, 1983.
[14] J. Murlis, J. S. Elkinton, and R. T. Cardé, "Odor plumes and how insects use them," *Ann. Rev. Entomol.*, vol. 37, pp. 505–532, 1992.
[15] W. Li, J. A. Farrell, and R. T. Cardé, "Tracking of fluid-advected odor plumes: Strategies inspired by insect orientation to pheromone," *Adapt. Behav.*, vol. 9, no. 3/4, pp. 143–170, 2001.
[16] J. A. Farrell, S. Pang, and W. Li, "Plume mapping via hidden Markov methods," *IEEE Trans. Syst., Man, Cybern.-B*, vol. 33, no. 6, pp. 850–863, 2003.
[17] J. A. Farrell, J. Murlis, W. Li, and R. T. Cardé, "Filament-based atmospheric dispersion model to achieve short time-scale structure of odor plumes," *Environt. Fluid Mech.*, vol. 2, pp. 143–169, 2002.
[18] J. A. Farrell, W. Li, S. Pang, and R. Arrieta, "Chemical plume tracing experimental results with a REMUS AUV," in *MTS/IEEE Oceans*, 2003.
[19] K. R. Mylne, "Concentration fluctuation measurements in a plume dispersing in a stable surface layer," *Boundary-Layer Meteorol.*, vol. 60, pp. 15–48, 1992.
[20] O. G. Sutton, "The problem of diffusion in the lower atmos-phere," *Q. J. R. Meteorol. Soc.*, vol. 73, pp. 257–281, 1947.
[21] ——, *Micrometeorology*. New York: McGraw-Hill, 1953.
[22] F. W. Grasso, T. Consi, D. Mountain, and J. Atema, "Locating odor sources in turbulence with a lobster inspired robot," in *From Animals to Animats 4: Proc. 4th Int. Conf. Simulation of Adaptive Behavior*, P. Maes, M. J. Mataric, J.-A. Meyer, J. Pollack, and S. W. Wilson, Eds., 1996, pp. 104–112.
[23] J. H. Belanger and M. A. Willis, "Adaptive control of odor-guided location: Behavioral flexibility as an antidote to environmental unpredictability," *Adapt. Behav.*, vol. 4, pp. 217–253, 1998.
[24] J. H. Belanger and E. A. Arbas, "Behavioral strategies underlying pheromone-modulated flight in moths: Lessons from simulation studies," *J. Comparative Physiol. A-Sensory Neural Behavioral Physiol.*, vol. 183, no. 3, pp. 345–360, 1998.

[25] F. W. Grasso, T. R. Consi, D. C. Mountain, and J. Atema, "Biomimetic robot lobster performs chemo-orientation intur-bulence using a pair of spatially separated sensors: Progress and challenges," *Robot. Autonom. Syst.*, vol. 30, pp. 115–131, 2000.
[26] F. W. Grasso, "Invertebrate-inspired sensory-motor systems and autonomous, olfactory-guided exploration," *Biol. Bull.* , vol. 200, pp. 160–168, 2001.
[27] H. Ishida, Y. Kagawa, T. Nakamoto, and T. Moriizumi, "Odor-source localization in the clean room by an autonomous mobile sensing system," *Sens. Actuators B*, vol. 33, pp. 115–121, 1996.
[28] H. Ishida, T. Nakamoto, T. Moriizumi, T. Kikas, and J. Janata, "Plume-tracking robots: A new application of chemical sensors," *Biol. Bull.*, vol. 200, pp. 222–226, 2001.
[29] Y. Kuwana, S. Nagasawa, I. Shimoyama, and R. Kanzaki, "Synthesis of the pheromone-oriented behavior of silkworm moths by a mobile robot with moth antennae as pheromone sensors," *Biosens. Bioelectron.*, vol. 14, pp. 195–202, 1999.
[30] A. T. Hayes, A. Martinoli, and R. M. Goodman, "Distributed odor source localization," *IEEE Sensors*, 2002.
[31] M. T. Stacey, E. A. Cowen, T. M. Powell, E. Dobbins, S. G. Monismith, and J. R. Koseff, "Plume dispersion in a stratified, near-coastal flow: Measurements and modeling," *Continental Shelf Res.*, vol. 20, pp. 637–663, 2000.
[32] M. Arbib, "Perceptional structures and distributed motor control," in *Handbook of Physiology – The Nervous System II*, V. B. Brooks, Ed: American Physiological Society, 1981, pp. 1449–1480.
[33] V. Braintenberg, *Vehicles: Experiments in Synthetic Psychology*. Cambridge, MA: MIT, 1984.
[34] R. A. Brooks, "A robust layered control system for a mobile robot," *IEEE J. Robot. Automat.*, vol. RA-2, pp. 14–23, 1986.
[35] R. C. Arkin and R. R. Murphy, "Autonomous navigation in a manufacturing environment," *IEEE Trans. Robot. Automat.*, vol. 6, pp. 445–454, 1990.
[36] W. Li, C. Y. Ma, and F. M. Wahl, "A neuro-fuzzy system architecture for behavior-based control of a mobile robot in unknown environments," *Fuzzy Sets Syst.*, vol. 87, pp. 133–140, 1997.
[37] K. Berns, R. Dillmann, and R. Hofsteller, "An application of a backpropagation network for the control of a tracking behavior," in *Proc. IEEE Int. Conf. Robot. Automat.*, 1991, pp. 2426–2431.
[38] W. Li, "Fuzzy-logic-based reactive behavior control of an autonomous mobile system in unknown environments," *Eng. Applicat. Artif. Intell.*, vol. 7, no. 5, pp. 521–531, 1994.
[39] A. Saffiotti, E. H. Ruspini, and K. Konolige, "Blending reactivity and goal-directness in a fuzzy controller," in *Proc. IEEE Int. Conf. Fuzzy Syst.*, 1993, pp. 134–139.
[40] L. E. Dubins, "On curves of minimal length with constraint on average curvature, and with prescribed initial and terminal positions and tangents," *Amer. J. Math.*, vol. 79, pp. 497–516, 1957.

Jay A. Farrell (M'86–SM'97) received the B.S. degrees in physics and electrical engineering from Iowa State University, Ames, in 1986, and the M.S. and Ph.D. degrees in electrical engineering from the University of Notre Dame, Notre Dame, IN, in 1988 and 1989, respectively.

Between 1989–1994, he was a Principal Investigator on projects involving intelligent and learning control systems for autonomous vehicles at Charles Stark Draper Lab, Cambridge, MA. Now he is a Professor and former Chair of the Department of Electrical Engineering with the University of California, Riverside. His research interests include: identification and on-line control for nonlinear systems, integrated GPS/INS navigation, and artificial intelligence techniques for autonomous vehicles. He is the author of the book *The Global Positioning System and Inertial Navigation* (New York: McGraw-Hill, 1998) and more than 118 additional technical publications.

Dr. Farrell received the Engineering Vice President's Best Technical Publication Award in 1990, and Recognition Awards for Outstanding Performance and Achievement in 1991 and 1993.

Shuo Pang received the B.Eng. degree in electrical engineering from Harbin Engineering University, China, in 1997 and the M.S. degree in electrical engineering from University of California, Riverside, in 2001. Currently, he is a Ph.D. degree student at the University of California, Riverside.

His current research interests include hybrid electrical vehicles energy management system and artificial intelligence techniques for autonomous vehicles, i.e., autonomous vehicle chemical plume tracing, autonomous vehicle online mapping, and planning.

Wei Li (M'94) received the B.S. and M.S. degrees in 1982 and 1984, respectively, in electrical engineering from the Northern Jiaotong University, Beijing, P.R. China, and the Ph.D. degree in 1991 in electrical and computer engineering from the University of Saarland, Germany.

He was a faculty member with the Computer Science and Technology, Tsinghua University, from 1993–2001. In 2001, he became an Associate Professor of Computer Science at California State University, Bakersfield. His research interests are intelligent systems, robotics, fuzzy logic control and neural networks, multisensor fusion and integration, and graphical simulation.

Dr. Li received the 1995 National Award for Outstanding Postdoctoral Researcher in China and the 1996 Award for Outstanding Young Researcher at Tsinghua University. He was a Croucher Foundation Research Fellow (1996) at City University of Hong Kong and an Alexander von Humboldt Foundation Research Fellow at the Technical University of Braunschweig, Germany (1997–1998).